

Pragmatic Modeling of Dynamic Magnetization and Iron Loss in Grain-Oriented Steel Sheets

M. Petrun¹, *Member, IEEE*, S. Steentjes², K. Hameyer², *Senior Member, IEEE*, and B. Polajzer¹, *Member, IEEE*

¹Institute of Power Engineering, FERI, University of Maribor, SI-2000 Maribor, Slovenia

²Institute of Electrical Machines, RWTH Aachen University, D-52062 Aachen, Germany

This paper presents the extension of two one-dimensional lamination models with magnetic hysteresis to reproduce dynamic hysteresis loops and power loss in grain-oriented (GO) electrical steels. For this purpose the concept of magnetic viscosity is introduced in the model equations. The applicability and accuracy is demonstrated by means of two GO steels of different thickness at magnetizing frequencies up to 1000 Hz. Advantages and limits of the classical approach with and without viscosity and comparisons to measured data are discussed in detail.

Index Terms—Eddy current diffusion, magnetic hysteresis, magnetic power loss, saturation wave model, soft magnetic materials.

I. INTRODUCTION

SOFT magnetic steel is almost universally used for many contemporary electric devices, where both the non-oriented (NO) and grain oriented (GO) types are applicable for specific applications according to their advantageous properties. The need for accurate descriptions of dynamic magnetization curves under arbitrary magnetization conditions resulted in various magneto-dynamic models [1]–[4]. Although both types of soft magnetic steel sheets (SMSSs) exhibit specific properties such as saturation due to material properties and dynamic hysteresis due to induced eddy currents, the underlying mechanisms that result in the dynamic loop distortion are remarkably different [2], [5], [6].

The spatially random domain structure and the small grain size of NO materials allow one to treat their properties as almost homogeneous and isotropic. In this case, the classical Maxwell diffusion equation is an appropriate basis to describe the magnetization dynamics in which eddy currents are assumed to flow parallel to the surface of the sheet [1]–[3], [5], [6].

In contrast to NO steel sheets, GO sheets exhibit different (coarser) domain structure, where the individual domains and their influence on the magnetization dynamics cannot be neglected [2], [5], [6]. Due to different nature of magnetization, the classical one-dimensional (1-D) modeling approach used for NO steels is strictly physically speaking not adequate for predictions of magnetization dynamics in GO steel sheets. To adequately describe the basic physical processes in GO steels, a domain-based dynamic model of the SMSS should be applied [2]. However, avoiding potentially complex-dynamic domain models that represents the rigorous description of underlying phenomena, the classical modeling approach can be still adequate in applied engineering if the predictions of the model adequately satisfy the behavior of the GO SMSSs in a broad frequency range. Such a modeling approach can be tailored to describe the magnetization dynamics in magnetically anisotropic GO materials by additionally introducing

a time delay of the local magnetic flux density with respect to the magnetic field strength across the SMSS. Such time delay can be e.g. effectively achieved by introducing the so-called magnetic-viscosity field term in addition to the classical dynamic and static hysteresis magnetic field terms [2], [3].

The classical dynamic model extended with the magnetic viscosity was found to be adequate for prediction of the magnetization dynamics and power loss inside GO SMSSs [2]. The accuracy of the proposed model, however, is dependent on the increased complexity of the viscosity component that, besides, takes a complex identification process based on a huge amount of measured data. In this way, the complexity by not using a domain model was not really avoided, but rather transferred to the description of the magnetic-viscosity component of the magnetic field. The aim of this paper is therefore to analyze different possibilities of phenomenological descriptions of magnetization dynamics inside GO SMSSs by using different simple classical models extended by a basic viscosity model description. The simplicity of the proposed models is obtained by using a minimum set of constant parameters.

II. THEORETICAL BACKGROUND

The classical 1-D approximation, represented by the well-known Maxwell diffusion equation coupled to a non-linear (hysteretic) static material model, can be solved using various approaches [1], [2], [4], [5], [7]–[9]. All these approaches have a common feature; the excitation surface magnetic field strength $H_{\text{sur}}(t)$ is equal to the sum of a static field $H_{\text{stat}}(t)$ term due to the static non-linear (hysteretic) relationship and a dynamic field term $H_{\text{dyn}}(t)$ caused by induced macroscopic eddy currents, i.e. $H_{\text{sur}}(t) = H_{\text{stat}}(t) + H_{\text{dyn}}(t)$. The static field component can be calculated by $H_{\text{stat}}(B)$ using an adequate inverse static hysteresis model [1], [10].

A. Simplified Models of Dynamic Magnetization

The first simplified approach takes integral impact of induced eddy currents on the magnetic field. It links the magnetic field strength at the sheet surface $H_{\text{sur}}(t)$ and the mean magnetic flux density $\bar{B}(t) = \langle B(t, x) \rangle$ over its cross-section.

Manuscript received March 10, 2017; revised April 26, 2017
Corresponding author: Martin Petrun (email: martin.petrun@um.si).

Using this approximation, the non-linear skin effect inside the SMSS is neglected. Thus, it is limited to low excitation dynamics where the skin effect is negligible [2], [6], [8], [11]. This assumption is valid for SMSS that are thinner than the penetration depth of the magnetic field, hence this model is known as the thin-sheet model (TSM):

$$H_{\text{sur}}(t) = \bar{H}_{\text{stat}}(\bar{B}, t) + \frac{\sigma b^2}{12} \frac{d\bar{B}(t)}{dt}, \quad (1)$$

where b is the thickness and σ is the conductivity of the SMSS.

In the second simplified approach the non-linear constitutive relationship of the material is approximated by a step-like magnetization curve or hysteresis [2], [5], [7], [8]. This approach is known as the saturation-wave model (SWM):

$$H_{\text{sur}}(t) = \bar{H}_{\text{stat}}(\bar{B}, t) + \frac{\sigma b^2}{8} \frac{|\bar{B}(t) - \bar{B}(0)|}{B_M} \frac{d\bar{B}(t)}{dt}, \quad (2)$$

where $\bar{B}(t)$ and $\bar{B}(0)$ are the average magnetic flux density inside the SMSS and its value at the previous reversal points, respectively. B_M can be used as a phenomenological model parameter that is adjusted to partially compensate the deviation due to the assumed step-like magnetization curve [7]. Despite its simplicity, the SWM performs surprisingly well in an extended excitation dynamics range (including skin effect) [2], [7], [8].

B. Modeling Non-linear Skin Effect

Models that take into account the non-linear skin effect are more complex, because they generally require a spatial discretization of the SMSS [1], [4], [7]. One of the most recent approaches is the parametric magneto-dynamic (PMD) model that basically extends the idea of the TSM modeling approach to several slices [12]. The magnetic field inside individual slices is described by its average values of magnetic field strengths \bar{H}_s and flux densities \bar{B}_s (analogous to the TSM), where the variables in individual slices are coupled by a coupling matrix \mathbf{L} . The PMD model is fully described by a system of ordinary differential equations (ODEs):

$$\mathbf{H}_{\text{sur}}(t) = \bar{\mathbf{H}}_s(\bar{\mathbf{B}}_s, t) + \sigma b^2 \mathbf{L} \frac{d\bar{\mathbf{B}}_s(t)}{dt}, \quad (3)$$

where \mathbf{H}_{sur} is a vector of surface (excitation) magnetic field strengths and $\bar{\mathbf{H}}_s(\bar{\mathbf{B}}_s)$ is a vector of average magnetic field strengths \bar{H}_s as a hysteretic function of average magnetic flux densities \bar{B}_s inside individual slices. The size of the obtained ODE system depends on the spatial discretization (number of slices), which furthermore depends on the excitation dynamics [1], [11]. In the case when only one slice is needed, the PMD model gives the classical eddy-current approximation, i.e., the TSM (1).

C. Modeling Magnetic Viscosity Effects

Using static $H_{\text{stat}}(t)$ and dynamic $H_{\text{dyn}}(t)$ field components is often not sufficient to model the total magnetization inside various SMSS, especially when modeling materials with a coarser-grained structure [2], [6]. The additional phenomena resemble a viscous-like friction, therefore they can be

accounted for by introducing the so-called magnetic viscosity [2], [3]. The lag in the magnetic flux density $\bar{B}(t)$ behind the applied field $\bar{H}(t)$ caused by microscopic phenomena can be in general effectively described by:

$$H_{\text{sur}}(t) = \bar{H}_{\text{stat}}(\bar{B}, t) + \bar{H}_{\text{dyn}}(t) + \delta \left| g(\bar{B}) \frac{d\bar{B}(t)}{dt} \right|^{\frac{1}{\alpha}}, \quad (4)$$

where $g(\bar{B})$ represents an adequate function that controls the impact of the viscous term $\bar{H}_{\text{vis}}(t)$ (consequently the shape of the total dynamic loop), δ is a directional variable and α a model parameter. By introducing a complex function $g(\bar{B})$ and upgrading the parameter α to be dependent on \bar{B} , virtually any dynamic loop shape can be reproduced [2], [3]. However, using such functions increases the complexity of the model and its parameter identification, whereas its practical value is significantly reduced. To keep the viscosity term $\bar{H}_{\text{vis}}(t)$ simple, the function $g(\bar{B})$ can be simplified as (5)

$$\bar{H}_{\text{vis}}(t) = \delta \left| R_m \left(1 - \frac{\bar{B}^2}{B_{\text{sat}}^2} \right) \frac{d\bar{B}(t)}{dt} \right|^{\frac{1}{\alpha}}, \quad (5)$$

where R_m is a constant model parameter and B_{sat} is the saturation flux density of the SMSS [8]. The viscosity component $\bar{H}_{\text{vis}}(t)$ can be added to all discussed classical dynamic models, whereas in the case of the PMD model $\bar{H}_{\text{vis}}(t)$ is applied in each slice individually.

III. RESULTS

Both the SWM as well as the PMD model were implemented as voltage driven versions (coupled to an model of the excitation winding [1], [10], [12]) by using the commercial Matlab/Simulink software package. The static hysteretic relationship of the material was taken into account by

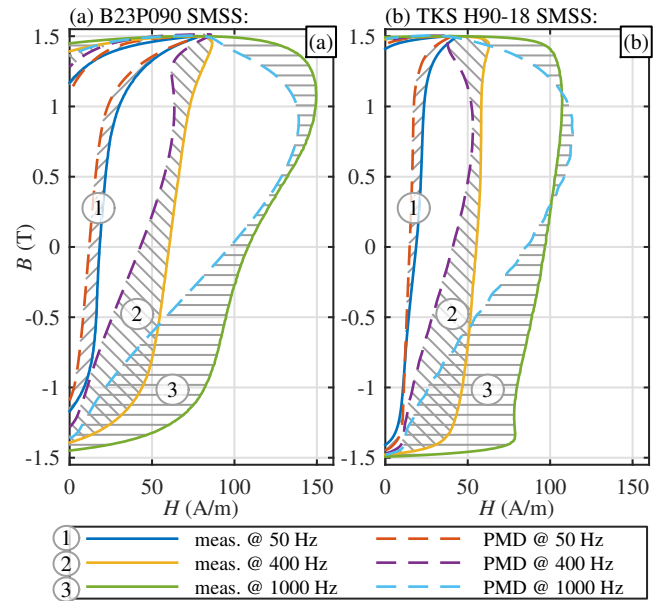


Fig. 1. Comparison of measured (continuous lines) and calculated (dashed lines) dynamic hysteresis loops using sinusoidal excitation at $B_{\text{max}} = 1.5$ T for: a) B23P090 and b) TKS H90-18 steel grades. Calculations were performed using the PMD model (classic eddy currents) with physical (real) SMSS parameters, whereas hatched areas ①, ② and ③ represent deviations between predicted and measured magnetization curves.

using the Tellinen hysteresis model [10]. The analysis was performed for two GO steel grades, namely 0.23-mm thick *B23P090* and 0.18-mm thick *TKS H90-18* steel grade. The used samples exhibited significantly different magnetic properties (i.e. static hysteresis loops), however equal measured conductivity $\sigma = 2.07 \cdot 10^6$ S/m. The discussed samples were experimentally tested using sinusoidal excitation waveforms in the frequency range up to $f = 1$ kHz and maximum magnetic flux density range up to $B_{\max} = 1.6$ T using a standard Epstein frame experimental setup.

A. Performance of the Classical Models

First the pure classical models (neglecting the $H_{\text{vis}}(t)$ viscosity component) were tested, where real (physical) measured parameters of the discussed samples were used. The results for the PMD model at $B_{\max} = 1.5$ T and frequencies $f = 50$ Hz, $f = 400$ Hz and $f = 1$ kHz versus measurements are shown in Fig. 1.

Obtained theoretical results in Fig. 1 show significantly different dynamic loops compared to the measured ones for both SMSSs, in particular at higher frequencies. This fact confirms that the classical modeling approach is inadequate and physically not correct when modeling GO materials [6]. Furthermore, it is clear that complex functions $g(\vec{B})$ are required when using the viscosity extension to disguise the incorrectness of the classic modeling approach, as the path of obtained magnetization trajectories differs significantly in comparison to the measured ones [2], [3]. Hatched areas ② and ③ in Fig. 1 show highly variable deviations of predicted classical dynamic magnetization curves, which could be adequately minimized by using complex functions $g(\vec{B})$.

However, from the calculated results it can also be seen, that at low excitation frequencies [e.g. $f = 50$ Hz; hatched area ①

in Fig. 1(a)] the magnetization trajectories flow almost parallel to each other, where the predicted dynamic loops are narrower than measured ones. Such model deficiency can be elegantly eliminated by using the $\vec{H}_{\text{vis}}(t)$ component described by (5), where constant parameters R_m , B_{sat} and α can be used.

B. Pragmatic Generalization of the Classical Models

It was found that the basic extension approach where constant viscosity parameters are used can be generalized also for higher frequencies, where the predicted classical magnetization trajectories were not parallel to the measured ones. When the PMD model is used, the shape of the dynamic loops (inclination of magnetization trajectories) can be adjusted by changing the conductivity σ of the SMSSs. By adjusting σ adequately, the PMD model predicts loops that are almost parallel to the measured ones in an extended frequency range. In this way, the deficiencies can be covered using a simple viscous extension. Due to the fact that the classical modeling approach is not physically correct, the physical parameters such as σ lose their original purpose and can be therefore regarded as a free model parameter.

To validate the developed approach, the PMD model with applied viscous extension was tested versus measurements. At first, parameter α was set to $\alpha = 2$ in order to keep the number of parameters to identify low and to keep consistency with the statistical theory of excess loss [2], [5]. Parameter B_{sat} represents the saturation magnetic flux density of the material and was also preset to $B_{\text{sat}} = 2$ T. Applying discussed assumptions, only two parameters are left to identify: σ , which controls the basic expansion and frequency-dependent inclination of the hysteresis loops, and R_m , which controls their excess expansion.

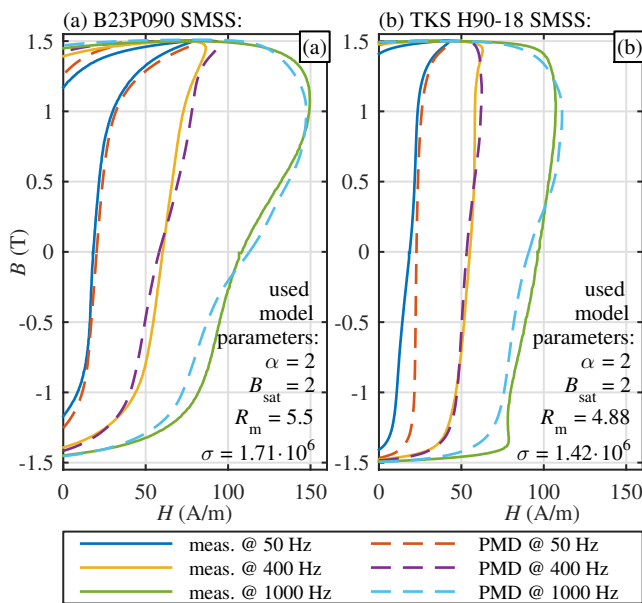


Fig. 2. Comparison of measured (continuous lines) and calculated (dashed lines) dynamic hysteresis loops using sinusoidal excitation at $B_{\max} = 1.5$ T for: a) *B23P090* and b) *TKS H90-18* steel grades. Calculations were performed using the PMD model extended with magnetic viscosity where partially non-physical constant model parameters were applied.

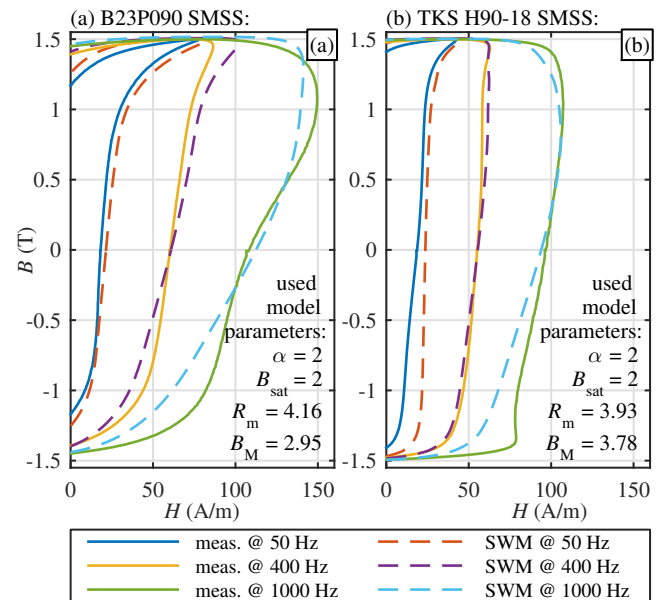


Fig. 3. Comparison of measured (continuous lines) and calculated (dashed lines) dynamic hysteresis loops using sinusoidal excitation at $B_{\max} = 1.5$ T for: a) *B23P090* and b) *TKS H90-18* steel grades. Calculations were performed using the SWM extended with magnetic viscosity where partially non-physical constant model parameters were applied.

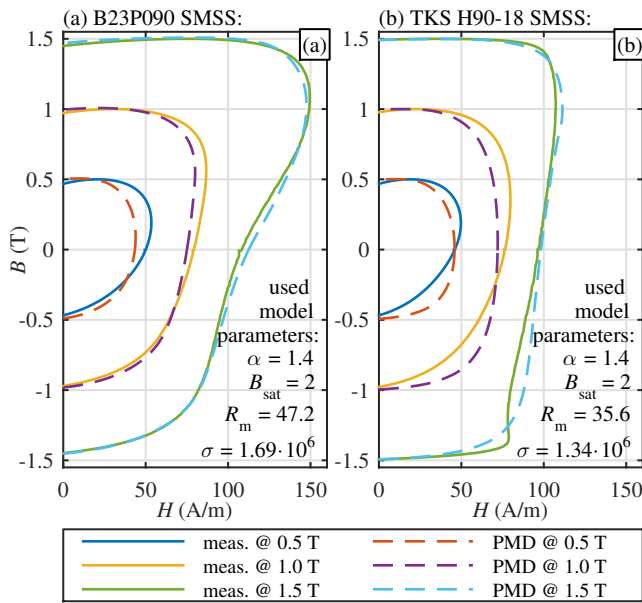


Fig. 4. Comparison of measured (continuous lines) and calculated (dashed lines) dynamic hysteresis loops using sinusoidal excitation of $f = 1$ kHz at different B_{\max} for: a) *B23P090* and b) *TKS H90-18* steel grades. Calculations were performed using the PMD model extended with magnetic viscosity where non-physical constant model parameters were applied.

The parameters σ and R_m were determined by using the optimization method differential evolution, where only measured major loops (i.e. at $B_{\max} = 1.6$ T) were used for identification. The parameters were optimized in such a way that the normalized-root-mean-square (NRMS) error ϵ between the measured $[H_m(B_m)]$ and calculated $[H_c(B_c)]$ magnetization curves was minimized. Due to the use of voltage driven models, both B_c and H_c can deviate from the measured values, hence ϵ for individual loop was defined by:

$$\epsilon = \sqrt{\frac{1}{n} \sum_{i=1}^n \left(\left(\frac{B_{m,i} - B_{c,i}}{\Delta B_m} \right)^2 + \left(\frac{H_{m,i} - H_{c,i}}{\Delta H_m} \right)^2 \right)}, \quad (6)$$

where n denotes the number of evaluated points and $\Delta B_m = 2B_{\max}$ and $\Delta H_m = 2H_{\max}$ are data ranges of the measured hysteresis loops. In the optimization procedure hysteresis loops at three different frequencies (i.e. 50, 400 and 1000 Hz) were taken into account simultaneously to obtain the best fit over the analyzed frequency range. It is worthwhile to note that satisfactory results were also obtained, when the parameters were optimized based only on major hysteresis loop at one frequency.

Obtained results for both GO samples are presented in Fig. 2. The results confirm that the validity of the model can be extended to a much broader frequency range by identifying only two parameters, where predicted results agree with the measurements reasonably well. The identified value of σ was found to be slightly lower than the physical one, which in turn decreased the induced eddy currents and diffusion of the magnetic field predicted by the classic component.

The same approach was tested also in the case when SWM is coupled to the simple viscous extension. According to

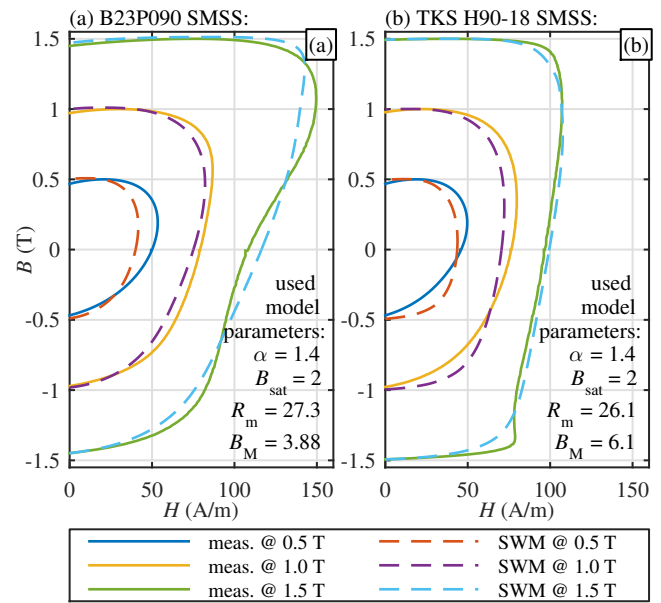


Fig. 5. Comparison of measured (continuous lines) and calculated (dashed lines) dynamic hysteresis loops using sinusoidal excitation of $f = 1$ kHz at different B_{\max} for: a) *B23P090* and b) *TKS H90-18* steel grades. Calculations were performed using the SWM extended with magnetic viscosity where non-physical constant model parameters were applied.

(2), the inclination of the predicted loop can be equivalently controlled either adjusting σ or B_M . As B_M is usually adjusted to compensate the deviation of the step-like magnetization curve from the non-linear one [7], [8], it was selected to control also the basic inclination, where σ was left at its measured (physical) value. Consequently only B_M and R_m were optimized in an analogous way to the previously discussed PMD case. The results are presented in Fig. 3. The accuracy of predicted dynamic loops in this case is slightly lower compared to the extended PMD model (Fig. 2), however still reasonably accurate for the use in applied engineering.

Although the minimum set of parameters to optimize has given reasonably accurate results, this set can also be increased. In the next step also the influence of α was analyzed. The performed sensitivity analysis has shown that when α was decreased, R_m was increased, as α and R_m are interdependent according to (5). By decreasing α also slightly better accuracy of both models was obtained, as shown in Fig. 4 and Fig. 5. It is worthwhile to note that the value α was never identified to be less than 1.3 when using α in the optimization procedure.

In Fig. 4 and Fig. 5 it is furthermore shown that the accuracy of the predicted loops decreases when predicting symmetrical minor hysteresis loops. However, the accuracy is still reasonably accurate and could be potentially improved if some minor loops were taken into account when identifying the parameters.

Finally, the power losses in the analyzed maximum flux density and frequency ranges were calculated and compared to the measured ones. The comparison is presented in Tab. I. The calculated (P_{PMD} and P_{SWM}) agree with measured power losses P_m and furthermore confirm previously obtained results. The losses (reflecting in areas of the loops) agree very well at higher B_{\max} , where the agreement is slightly decreased with

TABLE I
COMPARISON OF MEASURED AND CALCULATED POWER LOSS

f [Hz]	B23P090:				TKS H90-18:		
	B_{max} [T]	P_m	P_{PMD}	P_{SWM}	P_m	P_{PMD}	P_{SWM} [W/kg]
50	0.5	0.062	0.078	0.081	0.073	0.138	0.141
	1.0	0.252	0.256	0.271	0.253	0.343	0.353
	1.5	0.601	0.575	0.624	0.580	0.654	0.681
400	0.5	1.90	1.71	1.66	1.80	2.11	2.09
	1.0	6.87	6.17	6.21	6.17	6.38	6.42
	1.5	14.83	14.27	14.77	13.86	13.59	13.83
1000	0.5	8.80	8.03	7.35	8.10	8.65	8.25
	1.0	30.38	29.32	28.43	28.27	28.11	27.36
	1.5	70.70	70.93	70.26	61.62	62.46	61.74

decreasing B_{max} . To increase the accuracy in the latter region, the optimization procedure should be extended to include also symmetric minor loops.

C. Comparison and Performance of Extended Models

When comparing both discussed models, the SWM model predictions of magnetization curves are in general slightly less accurate. However, the SWM model in turn does not depend on discretization and is therefore simpler. Hence, the required discretization of the PMD model was analyzed. It was found out that by adding the viscosity term, the required discretization of the PMD model to accommodate the non-linear diffusion significantly decreases whereas the stability of numerical integration is increased. This result corresponds with findings in [3].

To adequately calculate the dynamic loops just two slices were sufficient, as shown in Fig. 5. By increasing the discretization to three slices only slightly better results were obtained, whereas increasing the number of slices over five was not even more noticeable. In comparison with classical PMD without viscosity at least 20 slices were used when calculating *TKS H90-18* samples in Fig. 1(b), where still oscillations due to spatial discretization of the PMD model were visible. The complexity of the PMD model is heavily decreased when applying the viscosity term, hence the PMD approach is not significantly more complex than the SWM approach. It is however very interesting that when the PMD model is simplified to only one slice (TSM model), the results become inadequate. The obtained results suggest that the domain-dynamics effects in GO steels remarkably resemble somewhat damped effects of non-linear skin effect in NO sheets. Consequently the classical models that account for the non-linear skin effect (e.g. the SWM or PMD model) represent a much more adequate basis for phenomenological modeling of GO steel sheets in comparison to models where skin effect is neglected (e.g. TSM).

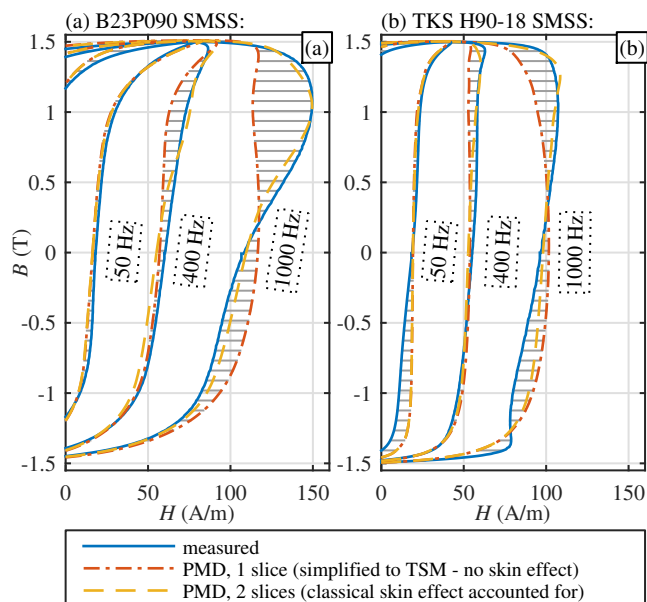


Fig. 6. Comparison of measured and theoretical dynamic magnetization curves for sinusoidal excitation at maximum average flux densities of $B_{max} = 1.5$ T when applying different spatial discretization of the PMD model. Hatched areas show significant deviations of predicted loops at higher frequency when the skin effect is not accounted for in the PMD model.

IV. CONCLUSION

In this paper a pragmatic modeling approach to predict magnetization dynamics and power loss inside GO SMSSs is proposed. The presented modeling approach is based on a simple magnetic viscous-like extension of classical dynamic models that were validated for NO SMSSs. The model has been tested on two GO electrical steels with different thickness and in each case a striking accuracy is apparent. The main properties of the presented models are their simplicity, ease of implementation, computational performance and simple identification. This makes the model suitable for use in applied engineering.

ACKNOWLEDGMENT

This work was supported in part by ARRS, Project Number P2-0115. The work of S. Steentjes is supported by the DFG and carried out in the research project “Improved modeling and characterization of ferromagnetic materials and their losses”.

REFERENCES

- [1] M. Petrun, S. Steentjes, K. Hameyer, and D. Dolinar, “One-Dimensional Lamination Models for Calculating the Magnetization Dynamics in Non-Oriented Soft Magnetic Steel,” *Magnetics, IEEE Transactions on*, vol. 52, no. 3, pp. 1–4, March 2016.
- [2] S. E. Zirka, Y. I. Moroz, P. Marketos, A. J. Moses, D. C. Jiles, and T. Matsuo, “Generalization of the Classical Method for Calculating Dynamic Hysteresis Loops in Grain-Oriented Electrical Steels,” *IEEE Transactions on Magnetics*, vol. 44, no. 9, pp. 2113–2126, Sept 2008.
- [3] S. E. Zirka, Y. I. Moroz, P. Marketos, and A. J. Moses, “Viscosity-based magnetodynamic model of soft magnetic materials,” *IEEE Transactions on Magnetics*, vol. 42, no. 9, pp. 2121–2132, Sept 2006.
- [4] Y. Shindo, T. Miyazaki, and T. Matsuo, “Cauer circuit representation of the homogenized eddy-current field based on the legendre expansion for a magnetic sheet,” *IEEE Transactions on Magnetics*, vol. 52, no. 3, pp. 1–4, March 2016.

- [5] G. Bertotti, *Hysteresis in Magnetism: For Physicists, Materials Scientists, and Engineers*, ser. Academic Press Series in Electromagnetism. Academic Press, 1998.
- [6] S. Zirka, Y. Moroz, S. Steentjes, K. Hameyer, K. Chwastek, S. Zurek, and R. Harrison, "Dynamic magnetization models for soft ferromagnetic materials with coarse and fine domain structures," *Journal of Magnetism and Magnetic Materials*, vol. 394, pp. 229 – 236, 2015.
- [7] M. Petrun, S. Steentjes, K. Hameyer, and D. Dolinar, "Modeling of magnetization dynamics using saturation wavefronts," *IEEE Transactions on Magnetics*, vol. PP, no. 99, pp. 1–1, 2016.
- [8] S. Steentjes, S. E. Zirka, Y. E. Moroz, E. Y. Moroz, and K. Hameyer, "Dynamic Magnetization Model of Nonoriented Steel Sheets," *IEEE Transactions on Magnetics*, vol. 50, no. 4, pp. 1–4, April 2014.
- [9] E. Dlala, "A Simplified Iron Loss Model for Laminated Magnetic Cores," *IEEE Transactions on Magnetics*, vol. 44, no. 11, pp. 3169–3172, Nov 2008.
- [10] S. Steentjes, K. Hameyer, D. Dolinar, and M. Petrun, "Iron-loss and magnetic hysteresis under arbitrary waveforms in no electrical steel: A comparative study of hysteresis models," *IEEE Transactions on Industrial Electronics*, vol. 64, no. 3, pp. 2511–2521, March 2017.
- [11] M. Petrun, S. Steentjes, K. Hameyer, J. Ritonja, and D. Dolinar, "Effects of saturation and hysteresis on magnetization dynamics: Analysis of different material models," *COMPEL - The international journal for computation and mathematics in electrical and electronic engineering*, vol. 34, no. 3, pp. 710–723, 2015.
- [12] M. Petrun, V. Podlogar, S. Steentjes, K. Hameyer, and D. Dolinar, "A Parametric Magneto-Dynamic Model of Soft Magnetic Steel Sheets," *Magnetics, IEEE Transactions on*, vol. 50, no. 4, pp. 1–4, April 2014.